OFFICE OF NAVAL RESEARCH

TECHNICAL REPORT

FOR

Grant N00014 91 J 1035

R & T Code 413302S

Technical Report No. 15

High-valent Oxo, Methoxorhenium Complexes: Models for Intermediates and Transition States in Proton-coupled Multi-electron Transfer Reactions

M.S. Ram, Lisa M. Skeens-Jones, Christopher S. Johnson,
Xiao Lian Zhang and Joseph T. Hupp

Dept. of Chemistry
Northwestern University
Evanston, IL 60208

REPORT DOCUMENTATION PAGE

Form Approved
OMB No. 0704-0188

1. AGENCY USE ONLY (Leave Blank)	2. REPORT DATE	3. REPORT TYPE AND DATES COVERED
	May 30, 1993	Technical Report, June 1992-June 1993

4. TITLE AND SUBTITLE

High-valent Oxo,Methoxorhenium Complexes: Models for Intermediates and Transition States in Proton-coupled Multi-electron Transfer Reactions

5. FUNDING NUMBERS

G.N00014-91-J-1035

6. AUTHOR(S)

M.S. Ram, Lisa M. Skeens-Jones, Christopher S. Johnson, Xiao Lian Zhang and Joseph T. Hupp

7. PERFORMING ORGANIZATION NAME(S) AND ADDRESS(ES)

Department of Chemistry
Northwestern University
2145 Sheridan Road
Evanston, IL 60208

8. PERFORMING ORGANIZATION REPORT NUMBER

15

9. SPONSORING/MONITORING AGENCY NAME(S) AND ADDRESS(ES)

Office of Naval Research
Chemistry Division
800 North Quincy Ave.
Arlington, VA 22217-500

10. SPONSORING/MONITORING AGENCY REPORT NUMBER

11. SUPPLEMENTARY NOTES

12a DISTRIBUTION AVAILABILITY STATEMENT

12b DISTRIBUTION CODE

13. ABSTRACT *(Maximum 200 words)*

Abstract: trans-Dioxorhenium(V) tetrapyridyl species are currently under active investigation as model systems for interfacial two-electron, two-proton transfer reaction sequences (Jones-Skeens, et al. Inorg.Chem. 1992, 31, 3879). We now find that the corresponding oxo,methoxo complexes can be prepared from the dioxo species and methyl trifluoromethanesulfonate. The new complexes behave nearly identically to the analogous oxo,hydroxo complexes — with one important exception: CH_3^+, unlike H^+, does not dissociate from the oxo ligand. As a direct consequence, the usually elusive rhenium oxidation state, IV, is stabilized with respect to redox disproportionation and is observable for several complexes at high pH. The ability to detect this state, in turn leads to: 1) direct access to the formal reduction potentials for the isolated 1e⁻ redox couples comprising the overall two electron transfer (key information for understanding multi-ET kinetics) 2) elucidation of the profound structural and energetic consequences of the initial protonation (methylation) step in the dioxorhenium(V) reduction kinetics, 3) estimates for pK_a of $(O)(HO)Re^{VI}L_4^{3+}$ (exceptionally negative), and 4) estimates for the first pK_a of $(HO)_2Re^{III}L_4^+$ (extremely large and positive).[2] The combination of (1) and (2), in principle, provides sufficient information to characterize completely the energetic accessibility of key intermediate species lying just before or just after the transition state for the two-electron, two-proton reduction of dioxorhenium(V) at electrochemical interfaces.

14 SUBJECT TERMS

15. NUMBER OF PAGES 48

16. PRICE CODE UL

17. SECURITY CLASSIFICATION OF REPORT	18 SECURITY CLASSIFICATION OF THIS PAGE	19 SECURITY CLASSIFICATION OF ABSTRACT	20. LIMITATION OF ABSTRACT
unclassified	unclassified	unclassified	UL

Introduction

High-valent metal-oxo and dioxo complexes often display an ability to accept multiple electrons as well as protons in a chemically reversible fashion at a single well-defined energy or potential,[1-7] e.g.:[8]

$$t\text{-}(O)_2\,Re^{V}(L)_4^{+} + 2e^{-} + 2H^{+} \xrightarrow{E_f} t\text{-}(HO)_2\,Re^{III}L_4^{+} \qquad (1)$$

The propensity towards multi-electron transfer (multi-ET) has motivated a number of attempts to exploit this class of systems in catalytic or redox-catalytic reaction sequences,[9] including water oxidation,[10] alkene epoxidation,[11] selective alcohol → ketone transformations,[12] etc.

In part because of their low formal reduction potentials (E_f), the dioxorhenium(V) complexes shown specifically in eq. 1 are *not* exceptionally useful as redox catalysts.[13] On the other hand, we have found them to be remarkably versatile model reactants for systematic studies of interfacial (i.e. electrochemical) multi-ET kinetics—an issue of obvious importance in redox-mediated catalysis, but also of more general significance.[14] Our preliminary experimental studies of reaction 1 (where L = pyridine (py) or any of several py derivatives) reveal that: (a) the kinetics of interfacial e^- and coupled H^+ transfer, in contrast to the thermodynamics, necessarily involve sequential, stepwise transfer (see Scheme I), (b) rapid, uphill protonation precedes the initial reduction step, and (c) depending on the exact circumstances, either the first (Re(V→IV)) or second (Re(IV→III)) redox step can be rate controlling.[15]

SCHEME I

$$t\text{-}(O)_2\,Re^{V}L_4^{+} + H^{+} \longrightarrow t\text{-}(O)(HO)\,Re^{V}L_4^{2+} \quad (2)$$

$$t\text{-}(O)(HO)\,Re^{V}L_4^{2+} + e^{-}(electrode) \longrightarrow t\text{-}(HO)(O)\,Re^{IV}L_4^{+} \quad (3)$$

$$t\text{-}(O)(HO)\,Re^{IV}L_4^{+} + e^{-}(electrode) \longrightarrow t\text{-}(HO)(O)\,Re^{III}L_4^{0} \quad (4)$$

$$t\text{-}(O)(HO)\,Re^{III}L_4^{0} + H^{+} \longrightarrow t\text{-}(HO)_2\,Re^{III}L_4^{+} \quad (5)$$

Thus, the singly protonated form of Re^{IV} can be regarded as the species lying either just after or just before the two-electron, two-proton transfer reaction transition state.[16]

Obviously, considerable mechanistic insight could be derived if this "near transition state" species could be isolated and characterized. Unfortunately Re^{IV} is unstable towards disproportionation (eq. 6) at all accessible pH's:[4a,d]

$$2\ t\text{-}(O)(HO)\,Re^{IV}L_4^{+} \longrightarrow t\text{-}(O)_2\,Re^{V}L_4^{+} + t\text{-}(HO)_2Re^{III}L_4^{+} \quad (6)$$

We wish to report here, however, the synthesis and characterization of a family of rhenium complexes which display, at high pH's, the elusive oxidation state IV. The new compounds are oxo, methoxo analogues of the dioxorhenium species. Remarkably, the methyl group behaves like a non-labile proton, providing in effect, spectroscopic and electrochemical access to the key intermediate species *t*-

$(O)(HO)Re^{V}L_4^{2+}$ and *t*-$(O)(HO)Re^{IV}L_4^{+}$. This in turn, leads to: 1) direct access to the formal potentials (E_f) for the isolated 1e⁻ redox couples comprising the overall 2 electron transfer,[17] 2) elucidation of the profound structural and energetic consequences of the initial protonation step in Scheme I, 3) estimates for the pK_a of $(O)(HO)Re^{VI}L_4^{3+}$ (exceptionally negative), and 4) estimates for the first pK_a of $(HO)_2Re^{III}L_4^{+}$ (extremely large and positive). Besides its obvious relevance to multi-ET kinetics, item (2) is also clearly pertinent to current studies of photoinitiated proton transfer, and especially back H^+ transfer,[18,19] e.g.:

$$t\text{-}(O)_2\,Re\,L_4^{+} \xrightarrow{h\nu} t\text{-}(O)_2\,Re\,L_4^{+\bullet} \xrightarrow{H^{\bullet}}$$

$$t\text{-}(O)(HO)\,Re\,L_4^{2+\bullet} \longrightarrow t\text{-}(O)(HO)\,Re\,L_4^{2+} \longrightarrow t\text{-}(O)_2Re\,L_4^{+} + H^{\bullet} \qquad (7)$$

Items (3) and (4), on the other hand, are perhaps most significant in the context of possible mechanisms for *trans*-dioxorhenium-based oxidative[13] and reductive[4a] electrocatalytic reactions, respectively.

Experimental Section

Materials. Tetrabutylammonium hexafluorophosphate ($TBAPF_6$) was prepared from HPF_6 and the corresponding bromide salt, and purified by recrystallization (3x). Ammonium hexafluorophosphate (95%) was purchased from Aldrich and used as received. Reagent grade CH_2Cl_2 was dried over alumina. All other starting materials were reagent grade chemicals from Aldrich or

Mallinckrodt and were used without further purification. Aqueous solutions were prepared by using water from a Milli-Q purification system.

Metals Complexes. The new compounds were derived in each case from related *trans*-$(O)_2ReL_4^+$ species, whose syntheses have already been described.[20] Abbreviations for L: dmap = 4-dimethylaminopyridine, 4-pyrrolidinopyridine = pyrrpy, MeOpy = 4-methoxypyridine, Me_2py = 3,4-dimethylpyridine (3,4-lutidine), Me-py = 4-methylpyridine and py = pyridine.

***trans*-[(O)(MeO)Re(dmap)]$(PF_6)_2$.** 1.2 g of $[(O)_2Re(dmap)]Cl$ was dissolved in 100 ml dry CH_2Cl_2. 10 g methyl trifluoromethanesulfonate was added and the solution was stirred at room temperature for 30 min. As the reaction proceeded, the color turned from yellow to purple and the solution became homogenous. Rotary evaporation of solvent at 35°C gave an oil which was then dissolved in 10 ml methanol. Addition of 10 ml of saturated NH_4PF_6 solution, followed by 200 ml of ether caused precipitation. The crude product was collected on a glass frit and washed with 2 x 30 ml of toluene and 3 x 40 ml of ether/ethanol. The compound was purified by doubly chromatographing on alumina with 98:2 CH_2Cl_2:isopropanol, and isolated by addition of ether. Yield (multiple syntheses): 20-60%. Anal. found: C, 34.6; H, 4.27; N, 10.63; F, 22.8; P, 6.16. Calcd.: C, 34.4; H, 4.25; N, 11.0; F, 22.8; P, 6.21. ^{1}H-NMR (acetone-d_6)(ppm): 7.86(d,8H), 3.93(s,3H), 3.33(s,24H). ^{13}C-NMR (acetone-d_6)(ppm): 157.4, 152.3, 110.0, 39.8.

***trans*-[(O)(MeO)Re(MeOpy)$_4$](PF$_6$)$_2$.** This complex was prepared in a similar fashion, except with $[(O)_2Re(MeOpy)_4]Cl$ as a starting material. The complex was

purified by twice passing a CH_2Cl_2 solution through a silica gel column initially prepared with CH_2Cl_2. Acetone, however, was used as the eluent. Addition of ether immediately precipitated the light purple product. Yield (multiple syntheses): 15-53%. Anal. found: C, 31.29; H, 3.21; N, 5.80. Calcd.: C, 31.29; H, 3.25; N, 5.83. ^{1}H-NMR (acetone-d_6)(ppm): 8.40(d,8H), 7.39(d,8H), 4.14(s,15H).

***trans*-[(O)(MeO)Re(py)$_2$(dmap)$_2$](PF$_6$)$_2$.** $[(O)_2Re(py)_2(dmap)_2]Cl$ was dissolved in 100 ml dry CH_2Cl_2 and reacted with 10 g of methyl trifluoromethanesulfonate. The yellow/brown reaction mixture was stirred for 1 hour. 1 g of $TBAPF_6$ was added to the resulting red/purple solution. The crude product was precipitated by addition of 200 ml ether and then washed twice with toluene and twice with an ether/ethanol mixture. The compound was purified by twice passing a CH_2Cl_2 solution through a silica gel column, eluting with 90:10 CH_2Cl_2:isopropanol. Addition of ether precipitated a bright purple product. Yield (multiple syntheses): 7-50%. Anal. found: C, 32.11; H, 3.64; N, 8.90. Calcd.: C, 32.43; H, 3.59; N, 9.07. ^{1}H-NMR (acetone-d_6)(ppm): 8.65(d,4H), 8.32(t,2H), 8.00(t,4H), 7.93(d,4H), 6.88(d,4H), 4.15(s,3H), 3.31(s,12H).

***trans*-[(O)(MeO)Re(pyrrpy)$_4$](PF$_6$)$_2$.** This compound was prepared and isolated in an analogous fashion to $[(O)(OMe)Re(py)_2(dmap)_2](PF_6)_2$, except that $[(O)_2Re(pyrrypr)_4](PF_6)$ was used as a starting material. The complex was purified by doubly chromatographing on alumina with 95:5 CH_2Cl_2:ethanol. The dark purple product precipitated upon addition of ether. Yield (multiple syntheses): 65-75%. Anal. found: C, 40.66; H, 4.65; N, 9.91. Calcd.: C, 39.82; H, 4.61; N, 10.04.

^{1}H-NMR (acetone-d_6)(ppm): 7.84(d,8H), 6.80(d,8H), 3.92(s,3H), 3.66(t,16H), 2.15(q,16H).

***trans*-[(O)(MeO)Re(Me$_2$-py)$_4$](PF$_6$)$_2$.** 2.2 g of [(O)$_2$Re(Me$_2$-py)$_4$]Cl was dissolved in 80 ml dry CH_2Cl_2 and 4 g methyl trifluoromethanesulfonate was added to the solution. The reaction mixture was stirred for 2 hours—the solution slowly becoming more purple in color. 1 g of $TBAPF_6$ was added, followed by 200 ml of ether, to yield an oil. The oil was redissolved in acetone, then precipitated as a solid after addition of 300 ml of ether. The crude product was washed twice each with toluene, chloroform, and ether. The complex was purified by doubly chromatographing on silica with acetone as the eluent. The light pink/purple product was precipitated upon addition of ether. Yield (multiple syntheses): 8-28%. Anal. found: C, 36.20; H, 4.09; N, 5.64. Calcd.: C, 36.59; H, 4.13; N, 5.88. ^{1}H-NMR (acetone-d_6)(ppm): 8.40(s,4H), 8.33(d,4H), 7.67(d,4H), 4.31(s,3H), 2.70(s,12H), 2.23(s,12H).

***trans*-[(O)(MeO)Re(Me$_2$py)$_4$](CF$_3$SO$_3$)$_2$.** The preparation and purification of this complex was analogous to that described for the PF_6^- salt, but without the addition of $TBAPF_6$. Anal. found: C, 37.49; H, 3.80; N, 5.62. Calcd.: C, 38.79; H, 4.09; N, 5.84.

***trans*-[(O)(MeO)(Me-py)$_4$](PF$_6$)$_2$.** The preparation of this complex was analogous to the preparation of [(O)(OMe)Re(Me$_2$-py)$_4$](PF$_6$)$_2$, except that [(O)$_2$Re(Me-py)$_4$]Cl was reacted with 4 g of methyl trifluoromethanesulfonate. The complex was purified by chromatographing twice on through silica with 95:5 CH_2Cl_2:ethanol as

eluent. Addition of ether immediately precipitated the pale pink/purple product. Yield (multiple syntheses): 6-10%. Anal. found: C, 30.94; H, 3.26; N, 5.64. Calcd: C, 33.52; H, 3.49; N, 6.26. ^{1}H-NMR (acetone-d_6)(ppm): 8.52(d,8H), 7.77(d,8H), 4.27(s,3H), 2.79(s,12H).

Metathesis of selected complex salts to the BPh_4^- form was accomplished by dissolving the $[(O)(MeO)ReL_4](PF_6)_2$ form and TBA^+ BPh_4^- separately in acetone. Combining the solutions led immediately to precipitation of the desired complex salt, which was collected on a glass frit and rinsed with acetone. These salts were particularly useful for IR studies, in view of interferences by the hexafluorophosphate anion in the rhenium-oxygen region.

Measurements. UV-visible absorption spectra were obtained with a Cary 14 spectrophotometer that had been rebuilt by OLIS. Infrared spectra were obtained from KBr pellets by using a Mattson FTIR instrument. Raman spectra were obtained via continuous excitation at 457.9 and 514.5nm with either a Spectra Physics Series 2000 or an Ion Laser Technologies argon ion laser, as previously described. Additional measurements at 647.1 nm were made with a Spectra Physics Series 2000 Kr^+ source. Samples were dissolved in 52:48 methanol:water, placed in a spinning NMR tube, and configured in a 180° backscattering geometry.

Formal potentials were estimated by cyclic voltammetry by using a standard three-electrode configuration and instrumentation previously described. Working electrodes were generally glassy carbon disks (3mm diameter Tokai GC-205, or 1 mm diameter electrodes from Cypress Systems). All potentials are

referenced to a saturated (NaCl) aqueous calomel electrode (s.s.c.e.). Mixed solvents (50:50 CH_3CN:water) were an unavoidable necessity in most electrochemical experiments because of solubility problems in purely aqueous solutions. Conductivity and pH control were maintained with buffers at μ = 0.1 M or at the pH extremes with strong acid or bases, as outlined previously. Apparent pH's (designated pH*) were determined with a Beckman 31 pH meter and a Beckman Model 39386 combination electrode (or calculated as -log [H*] for pH*'s below 1.0).

X-ray Crystallography. Crystals of *t*-[(O)(MeO)Re(Me_2py)$_4$](CF_3SO_3)$_2$ suitable for x-ray crystallographic measurements were grown from slow diffusion of an acetone/ether solution. A pale purple, transparent, columnar crystal having the dimensions 0.490 x 0.082 x .042 mm was mounted on a glass fiber using oil (Paraton-N, Exxon). Measurements were made on an Enraf Nonius CAD4 diffractometer with graphite monochromated Mo Kα radiation. Cell constants and an orientation matrix were obtained from a least-squares refinement using the setting angles of 25 centered reflections in the range $18.1 < 2\Theta < 20.7°$. Based on the systematic absences of h01: $1 \neq 2n$ and OkO: $k \neq 2n$ the space group was unambiguously determined to be $P2_1/c$ (#14). The data were collected using the ω-,-Θ scan technique to a maximum 2Θ value of 47°. Of the 8228 reflections which were collected, 6231 were unique. The intensities of three standard reflections, which were measured after every 90 minutes of x-ray exposure time, remained constant throughout data collection indicating crystal and electronic stability (no

decay correction was applied). The linear absorption coefficient for Mo Kα is 32.0 cm^{-1}. An analytical absorption correction was applied which resulted in transmission factors from 0.76 to 0.87. A summary of the crystal structure is given in Table I.

The structure was solved using heavy atom methods (Patterson and Fourier techniques) and refined by full-matrix least squares refinement based on 3365 absorption corrected reflections with $I > 3\alpha(I)$ and 461 variable parameters. The non-hydrogen atoms were refined either anisotropically or isotropically to give final $R(F) = 0.047$ and $R_w(F) = 0.049$. TEXSAN 4.0 crystallographic software was used throughout the calculations.[21]

A pyridine ring of one of the lutidine ligands and a $CF_3SO_3^-$ anion were found to be disorded. In the pyridine ring the atoms N31 and C32A were not disordered and were in full population. The populations of the other disordered carbon atoms were 0.605 for C33A-C36A and 0.395 for C32B-C35B (C36B is C32A). The thermal parameters of the disorded carbon atoms were independently refined isotropically. The fluorine populations of the $CF_3SO_3^-$ anion were 0.638 for F11A-F13A and 0.362 for F11B-F13B and the oxygen populations were 0.441 for O11A-O13A and 0.559 for O11B-O13B. Group thermal parameters were isotropically refined for the fluorines and the oxygens. Tables of crystal data, positional parameters, thermal parameters, interatomic distances, bond angles, and structure factors are available as supplementary material.

Results

Synthesis. Our initial efforts to add CH_3^+ to dioxorhenium complexes emphasized CH_3I as the methylating agent. These efforts were completely unsuccessful. Also unsuccessful were subsequent attempts with an even more potent methylating agent, $CF_3SO_3CH_3$—at least when the methylation targets were *trans*-$(O)_2Re(py)_4^+$, *trans*-$(O)_2Re(py\text{-}x)_4^+$ (where x is an electron-withdrawing substituent), or any of several *cis*-dioxorhenium(V) complexes. We ultimately were successful, however, with *trans*-dioxorhenium targets featuring comparatively electron rich pyridyl ligands such as 3,4-dimethylpyridine and 4-dimethylaminopyridine. In addition, within the reactive subset we found that the extent of reactivity (i.e. the oxo, methoxo product yield) progressively increased with increasing (cumulative) py ligand substituent electron-donating strength (Me-py < Me_2py < MeOpy < dmap ≈ pyrrpy). Nevertheless, even with the constraint that electron-rich pyrridine ligands be used, a total of six new complexes proved accessible via the methyltriflate route:

$$t\text{-}(O)_2ReL_4^+ + CF_3SO_3CH_3 \longrightarrow t\text{-}(O)(MeO)ReL_4^{2+} + CF_3SO_3^- \qquad (8)$$

Crystallography. Definitive assignment of the new complexes as oxo, methoxo complexes was achieved by x-ray crystallography. The crystallographic studies, however, were not without their difficulties. Several compounds yielded crystals which diffracted, but whose structures could not be fully refined. One of

the partially refined structures was for [*t*-(O)(MeO)Re(py)$_2$(dmap)$_2$](PF$_6$)$_2$. Here the extent of refinement was sufficient, however, to establish that the dmap ligands are coordinated trans to each other.

A complete structure was ultimately obtained for [*t*-(O)(MeO)Re(Me$_2$py)$_4$] (CF$_3$SO$_3$)$_2$. An ORTEP drawing is shown in Figure 1. Selected bond distances and bond angles are listed in Table II. Notable features in comparison to dioxo complexes include: 1) elongation of the methylated oxygen-rhenium bond to 1.83Å (from ca. 1.77Å), 2) compression of the nonmethylated oxygen-rhenium bond to 1.69Å, and 3) constancy of the nitrogen-rhenium bond lengths (at ca. 2.14Å). If one accepts 1.77Å as a typical rhenium-oxygen double-bond length[23] and 2.04Å (i.e. the sum of covalent radii) as a reasonable single-bond length, then the structure suggests multiple bonding to both oxo ligands (bond orders of, say, 1.5 and 2.5 respectively). The Re-N bond lengths, on the other hand, are consistent with single-bond formation. One other structural feature of note is the nearly linear rhenium-oxygen-carbon configuration. On the basis of several literature precedents, we had expected an angle of ca. 120° to 145° for Re-O1-C1.[24] In any case, the more linear configuration here would be consistent again with rhenium-oxygen multiple bonding.

Electronic Absorption Spectra. Shown in Figure 2 are representative UV-visible absorption spectra for (O)(MeO)ReL$_4^{2+}$ and (O)(HO)ReL$_4^{2+}$. The similarities are striking, especially in comparison to the spectroscopy for the parent dioxo complex. On the basis of its low extinction coefficient, the broad feature near

530nm in the $(O)(MeO)ReL_4^{2+}$ spectrum is assigned as a d-d (or ligand-field) transition. (The corresponding feature in the dioxorhenium spectrum appears at 430nm). Note that the d-d transition is formally forbidden; evidently it borrows significant intensity from neighboring allowed transitions.[26] The oxo, methoxo complexes also exhibit an intense absorption anywhere between 280 and 315 nm. Assignment as metal-to-ligand (pyridine) charge transfer (MLCT) is made on the basis of: a) the appearance of an apparently related MLCT transition near 350 nm in the corresponding dioxo complexes (i.e 400 to 900 meV lower in energy), coupled with (i.e. correlated with) b) a 650 to 1100 mV increase in the Re(VI/V) potential following methylation. Finally, for some complexes a third feature near 260nm can be resolved. Almost certainly this feature is a pyridine ligand centered transition.

Table III shows that the electronic absorption spectrum displays a substantial pyridyl ligand dependence. Both the MLCT and d-d transitions shift towards higher energy as the ligand basicity[27] decreases. (In contrast, in the parent dioxo complexes only the d-d transition responds to ligand basicity variations.)[4d,f] Perhaps the most striking feature of Table III, however, is the very close parallel between $(O)(MeO)ReL_4^{2+}$ and $(O)(HO)ReL_4^{2+}$ spectra — both in terms of intensities and energetics. Clearly the electronic consequences of oxo ligand methylation are very well approximated by protonation. Finally we note that none of the oxo, methoxo complexes is detectably luminescent, even when irradiated in nonhydroxylic solvents — again reminiscent of oxo, hydroxo species.[18]

Vibrational Spectroscopy. Resonance Raman scattering (514.5nm excitation) from the weakly absorbing d-d transitions of a representative pair of oxo, methoxo complexes is illustrated in Figure 3. The spectra are essentially completely devoid of pyridyl-type vibrations, as one would expect for ligand-field transitions. Also missing from both spectra is the characteristic O=Re=O (symmetric) stretch at ca. 906 cm^{-1}.[5a,g] In its place is an intense band at ca. 955-960 cm^{-1}, which is almost certainly assignable as a metal-oxo stretch. The increase in frequency is noteworthy and is suggestive of rhenium-oxygen triple bond formation. (As we have noted elsewhere,[5g] strong enhancement of Re-O modes (and a decrease in Re-O bond order) is expected when an electron residing in d_{xy} (i.e. the tetrapyridylrhenium plane) is promoted to d_{xz} or d_{yz}.) Other prominent bands in Figure 3 are found at 768 cm^{-1} (tentatively assigned as the Re-OMe stretch), 1137 cm^{-1} (speculatively assigned as the C-O(methoxy) stretch), and 1077 cm^{-1} (origin unknown). The peaks assigned as Re≡O and C-O are also readily observable in IR spectra.

Aqueous Electrochemistry Shown in Figure 4 are representative background-subtracted cyclic voltammograms for the 2e⁻ reductions of *t*-$(O)_2Re(dmap)_4^+$ (eq. 1) and *t*-$(O)(MeO)Re(dmap)_4^{2+}$ (eq. 9). Two observations, in particular, are worth mentioning. First, oxo methylation shifts the Re(V/III) formal potential positive by roughly 200 mV (at $pH^* = 8$). Secondly, the

$$(O)(MeO)Re^{V}L_4^{2+} + 2\ e^- + H^+ \rightarrow (HO)(MeO)Re^{III}L_4^+ \qquad (9)$$

electrochemical kinetics (as measured by voltammetry peak separations) are substantially accelerated by methylation.

Returning to the first point, the observed thermodynamic differences between related $(O)(MeO)(O)ReL_4^{2+}$ and $(O)_2ReL_4^+$ reductions are significantly dependent upon the pH^* at which the observations are made. Figures 5 and 6 (middle) present plots of E_f versus pH^* ("Pourbaix plots") for the pair of complexes, *t*-$(O)_2Re(MeOpy)_4^+$ and *t*-$(O)(MeO)Re(MeOpy)_4^{2+}$. Over most of the available pH^* range, the dioxorhenium(V) reduction proceeds by the two electron, two proton reaction of eq. 1.[28] (The proton stoichiometries (p) for the redox reactions have been determined from the slopes of the Pourbaix plots (ca. 60mV in each case), where the slopes more generally will equal -59(p/n) mV per pH^* unit.) Below pH^* = 6, further reduction to Re(II) is detectable:[8]

$$(HO)_2Re^{III}L_4^+ + e^- + H^+ \rightarrow (H_2O)(HO)Re^{II}L_4^+ \qquad \textbf{(10)}$$

The oxo, methoxo complex differs from the dioxo complex in that: a) the Re(III/II) couple is not observed within the accessible solvent stability window (it is observed with other complexes), b) the Re(V/III) couple is accompanied by only a single proton transfer (eq. 11), and c) at pH^*'s above approximately 10, the V/III

$$(O)(MeO)Re^{V}L_4^{2+} + 2e^- + H^+ \rightarrow (HO)MeO)Re^{III}L_4^+ \qquad \textbf{(11)}$$

reaction separates into its component steps and the elusive Re(IV) state appears.

The portion of the Pourbaix plot above $pH^* \approx 10$ shows that the one-electron reduction reactions are:

$$(O)(MeO)Re^{V}L_4^{2+} + e^- \rightarrow (O)(MeO)Re^{IV}L_4^{+} \quad (12)$$

and

$$(O)(MeO)Re^{IV}L_4^{+} + e^- + H^+ \rightarrow (HO)(MeO)Re^{III}L_4^{+} \quad (13)$$

Extension of the studies to four of the five other $(O)(MeO)Re^{V}L_4^{2+}$ complexes has yielded the Pourbaix data shown in Figures 6 (top and bottom) and 7. Additional dioxo results (previously unpublished) are shown in figure 8. As one might expect, the general reactivity pattern is similar to that illustrated above. An instructive trend, however, is a shift in the Re(V/IV)/Re(IV/III) separation point towards higher pH^* values as the electron donating strength of the pyridyl ligand substituents is increased. Indeed, for the two most strongly donating substituents (dimethylamine and pyrrolidine; Figure 7) the separation point is shifted out of the available pH^* range (i.e. resolution of the single-electron reduction components is never seen). Comparison of the single-electron potentials for the other four complexes (Figures 6 and 7; Table IV) gives some insight: For the proton-*de*coupled Re(V/IV) reaction, the formal potential moves to more negative values as the substituent electron-donating strength is increased. This is consistent, of course, with the usual differential stabilization of the higher oxidation state by ligand electron-donation effects. For the Re(IV/III) couple, on the other hand,

there is almost no dependence of E_f on ancillary ligand identity. It is tempting, on the basis of our own previous work, to interpret the behavior in terms of "electron/proton compensation effects", i.e. offsetting effects due to simultaneous hydroxo ligand pK_a shifts and isolated electron-transfer potential shifts.[4c] Results presented in the next section, however, show that E_f(IV/III) is ligand insensitive (or nearly so) even when proton uptake is decoupled from the reduction reaction. In any case, the observation of understandable trends in the separated V/IV and IV/III potentials permits one to make reasonable guesses for the potentials in the two instances where separation is not seen.

Finally, attempts instead to *oxidize* the $(O)(MeO)Re^{V}L_4^{2+}$ species were frustrated by the onset of water oxidation at far positive potentials (however, see next section).

Electrochemistry: Nonaqueous Experiments. In an effort both to access the Re(VI/V) couple and to disconnect the Re(V) and Re(IV) reductions from proton uptake, a series of electrochemical measurements was made in dry acetonitrile. A cyclic voltammogram for a representative compound, $(O)(MeO)Re(MeOpy)_4^{+}$, is shown in Figure 9. Key features are a reversible one-electron oxidation (to Re(VI)) at +1.98 V (eq. 14) and consecutive, reversible[29] one-electron reductions at -0.81 and -1.78 V (eqs. 12 and 15). (Note that reaction 12 occurs at -0.81 V in 50:50 CH_3CN:H_2O as well; see above.) Attempts to extend the measurements to dioxo

$$t\text{-}(O)(MeO)Re^{VI}L_4^{3+} + e^{-} \rightarrow t\text{-}(O)(MeO)Re^{V}L_4^{2+} \qquad (14)$$

$$t\text{-(O)(MeO)Re}^{IV}L_4^{+} + e^{-} \rightarrow t\text{-(O)(MeO)Re}^{III}L_4^{0} \qquad (15)$$

compounds yielded well-defined Re(V) oxidations (see Table V), but ill-defined reductions.[30] In any case, generalized comparisons show: 1) that methylation substantially increases E_f(VI/V), and 2) that elimination of proton transfer substantially destabilizes the lowest oxidation states, thereby fully separating the V/IV and IV/III redox steps.

Extension of the electrochemical measurements to other oxo, methoxo compounds (Table V) shows that an enormous sensitivity to ancillary (i.e. pyridyl) ligand composition exists for E_f(VI/V). Figure 10 shows more clearly that the E_f variations are related to pyridyl ligand basicity (or equivalently, substituent electron-donating strength). For E_f(V/IV), the dependence on basicity is diminished by roughly two-fold, while for the IV/III reaction it is nearly absent (see Table V and fig. 9). The enhanced sensitivity of E_f(VI/V) can presumably be understood in terms of simple d-orbital occupancy effects. The electronic configuration of Re(V) is d^2, with both electrons confined to d_{xy}, i.e. the one d orbital coincident with the tetrapyridylrhenium plane. The energetics of conversion to d^1 should be exceptionally sensitive, therefore, to any factors influencing pyridyl nitrogen electron density.[5f] On the other hand, conversion to d^3 or d^4 (with occupancy of d_{xz} and/or d_{yz}) should be less strongly influenced. Still unclear, however, is why the d^2/d^3 and d^3/d^4 couples should differ so greatly in their response to substituent effects.

Discussion

The synthetic observations are clearly consistent with a simple electrophilic attack upon one of the two available, formally dinegative, oxo ligands as the mechanism for oxo, methoxo complex formation. Coordination to rhenium(V), of course, greatly diminishes the effective charges—and therefore the reactivity—at the oxo sites. The residual oxo charge density (and reactivity) evidently can be significantly manipulated, however, by manipulating the ancillary ligand identity. Indeed, the reactivity/residual-oxo-charge correlation is nicely illustrated, in a qualitative way, by the variation of reaction yield (see experimental section) with the corresponding *t*-(O)(HO)$Re^{V}L_4^{2+}$ pK_a (i.e. higher yields with higher pK_a's). The pK_a analogy is also instructive with regard to geometric effects: the cis complexes—which resist methylation—also show no propensity (in oxidation state V) towards protonation.[4b]

Carrying the protonation analogy further, the general absence of double protonation of the trans complexes in oxidation state V (even at extreme pH's) is paralleled synthetically by the absence of dimethoxo products. Inactivation following the initial methylation is a finding consistent with the available x-ray and Raman data for *t*-(O)(MeO)ReL_4^{2+} (above). These show that the second rhenium-oxygen bond acquires substantial triple bond character. Presumably the increase in bond order is accompanied by further diminution in ligand charge density, thereby transforming the oxo into an extremely poor target for electrophilic (i.e. CH_3^+) attack.

Perhaps more surprising than the formation of the rhenium alkoxides[31] is the persistence of these high-oxidation-state species through workup in aqueous solution and subsequent characterization in both strongly acidic and strongly basic aqueous environments. Evidently, the methoxy linkage is very much less polar (less ionic), and more covalent, than its coordinated O (formally 2-)/CH_3 (formally 1+) parentage would suggest.

Aqueous Electrochemistry. Clearly the most interesting and important electrochemical observation, from a mechanistic kinetics viewpoint, is the appearance of the key intermediate state, Re(IV), for several of the oxo, methoxo complexes at high pH*'s. To place this finding in perspective, however, it is necessary to consider first the redox behavior at lower pH*'s. Here the Pourbaix slopes are ca. 30mV and 60mV per pH* unit for the two-electron reductions of the oxo, methoxo- and dioxo-rhenium(V) complexes,[4a,c] respectively. The slope difference indicates that not only are the two sets of V/III formal potentials pH* dependent, but also their *differences* are pH* dependent. For example, the initially quite disparate (high pH*) potentials for $(O)(MeO)Re(Me_2py)_4^{2+}$ and $(O)_2Re(Me_2py)_4^{+}$ reduction (see Figures 6 and 8) eventually converge near pH* = 0. Importantly, this pH* value is essentially the value at which the dioxorhenium(V) compound becomes protonated and the reduction reaction becomes a two-electron, one-proton process (eq. 16). (The same is true for other oxo,methoxo/dioxorhenium pairs.) It follows then, that reactions 11 and 16

$$t\text{-}(O)(HO)Re^{V}L_4^{2+} + 2e^- + H^+ \rightarrow t\text{-}(HO)_2Re^{III}L_4^+ \quad (16)$$

have essentially identical thermodynamics — a result consistent with the nearly identical spectroscopic properties of $(O)(MeO)ReL_4^{2+}$ and $(O)(HO)ReL_4^{2+}$ species.

In view of both the redox energetics and the spectroscopy, we conclude that the methoxo ligand and complex can be viewed as essentially the equivalent of the hydroxo ligand and complex, with one important difference: the methyl cation (unlike the proton) is irreversibly bound.

This interpretation (or conclusion) has a number of interesting consequences. First, the substantial difference in oxo,methoxorhenium(V→III) versus dioxorhenium(V→III) electrochemical kinetics (Figure 4) can be taken as a direct measure of the kinetic cost of preequilibrium protonation (eq. 2) in the overall multielectron, multiproton sequence (Scheme I) for $(O)_2Re^{V}L_4^+$ reduction. A second point is that the $(O)(MeO)ReL_4^+$ species can be used to project *what would have occurred* energetically at higher pH*'s in the $(O)(HO)Re^{V}L_4^+$ reduction reaction, if the hydroxyl proton had not dissociated. The most obvious result is that for 4 of the 6 complexes the Re(V/IV) and Re(IV/III) processes would have separated. The availability of separate one-electron (or one-electron, one-proton) potentials is highly significant because it ultimately provides a basis for understanding the kinetically relevant stepwise energetics of the multi-ET processes. For example, from Figures 6 and 7 and related data for $(O)_2ReL_4^+$ species, one should be able to determine whether electrochemical reaction rates

measured at the two-electron reduction potential are actually occurring at a significant overpotential or at an underpotential with respect to the energetics of the rate-determining step. We intend to report elsewhere on detailed interpretations of multi-ET kinetics, using the stepwise thermodynamics. To make the point here, however, it may be sufficient to recognize that: 1) the observed V/III potentials are simply arithmetic means of V/IV and IV/III potentials, and 2) the latter can be obtained in a straightforward fashion at lower pH^*'s by extrapolation from higher pH^*'s.

Nonaqueous Electrochemistry. Like the high pH^* aqueous measurements, the E_f measurements in dry acetonitrile provide effective access to the isolated thermodynamics of reaction 3 (i.e. the rate determining step in the overall 2 electron, 2 proton reduction of dioxorhenium(V)). The isolated thermodynamics of an alternative rate determining step,[15] reaction 4, are provided (approximately) by the E_f for reaction 15. When combined with the available data for the pre-equilibrium protonation of Re(V) (eq. 2; Table VI), these measurements then permit the kinetically relevant multi-ET reaction energetics, up through transition-state precursor formation (i.e. either $(O)(HO)Re^{V}L_4^{+}$ or $(O)(HO)Re^{IV}L_4^{0}$), to be determined. Indeed, we are currently exploiting this information in the analysis of measured, pH-dependent, reaction kinetics.[32] In addition, $(O)(MeO)ReL_4^{n+}$ redox measurements in nonaqueous media — especially when combined with aqueous $(O)_2ReL_4^{+}$ measurements — offer a unique method for assessing proton binding strengths over an exceptionally wide range of pK_a's. The key, as suggested above, is to treat CH_3^{+} as a nonlabile surrogate for H^{+}, when

bound to an oxo group. We then can gain effective energetic access to such unlikely species as $(O)(HO)Re^{VI}L_4^{3+}$. Knowledge of the pH-independent reduction potential (as represented by the oxo, methoxo complex) may then be exploited in conjunction with the pH-independent dioxorhenium(VI/V) potential to yield relative pK_a's for hydroxo ligands in the Re(VI) and Re(V) oxidation states:

$$E_f(VI/V)(oxo, methoxo) - E_f(VI/V)(dioxo) \approx RT/nF \ln [K_a(VI)/K_a(V)] \qquad (17)$$

Eq. 17 shows that for a one-electron reaction, the formal potentials for the two types of redox complexes will differ by 59 mV (for n = 1) for each factor of 10 difference in acid (hydroxo ligand) dissociation constants. For the complexes examined here, the oxidation-state dependent pK_a's differ by 12 to 18 orders of magnitude (on the basis of potential differences of 750 to 1080 mV; see Table V). pK_a's for most of the rhenium(V) species have been reported previously.[4c] These range from +2.3 to approximately 0. The corresponding oxo,hydroxorhenium(VI) pK_a's (eq. 18), therefore, are estimated as -10 to -18! Furthermore, the most negative values (see Table VI) are associated (as one would expect) with the complexes containing the least strongly electron donating pyridine substituents.

$$t\text{-}(O)(HO)Re^{VI}L_4^{3+} \xrightarrow{K_a(VI)} t\text{-}(O)_2ReL_4^{2+} + H^+ \qquad (18)$$

Turning the analysis around, the extremely negative $(O)(HO)Re^{VI}L_4^{3+}$ pK_a's illustrate just how crucial ligand deprotonation is in the stabilization of the higher oxidation states of oxo/hydroxo/aquo complexes.

On the basis of eq. 18, we additionally conclude that dioxorhenium(VI)

complexes will almost certainly be *in*effective as redox catalysts. Although the range of available Re(VI/V) potentials is attractive from a thermodynamic standpoint (particularly for common organic oxidation targets such as alcohols and olefins), the remarkable lack of affinity of $(O)_2Re^{VI}L_4^{2+}$ for protons (together with the very limited capability of $(O)_2Re^{V}L_4^{+}$ to bind protons) would argue against the possibility of coupled proton transfer or even H-atom extraction mechanisms for catalytic oxidation. Instead, it would appear that dioxorhenium(VI) species are capable of functioning only as simple redox mediators (i.e. single electron transfer agents) towards most oxidation targets.

Returning to thermodynamics, the combined aqueous and nonaqueous redox data can also be used to estimate the first pK_a for $(HO)_2R^{III}L_4^{+}$:

$$t\text{-}(HO)_2Re^{III}L_4^{+} \xrightarrow{K_a(III)} t\text{-}(O)(HO)Re^{III}L_4^{0} + H^{+} \qquad \textbf{(19a)}$$

$$t\text{-}(HO)(MeO)_2Re^{III}L_4^{+} \xrightarrow{K_a(III)} t\text{-}(O)(MeO)Re^{III}L_4^{0} + H^{+} \qquad \textbf{(19b)}$$

We assume again that methoxo species (i.e., $(O)(MeO)Re^{III}L_4^{0}$ and $(HO)(MeO)Re^{III}L_4^{+}$) can function as surrogates for hydroxo species. We then observe that eq. 19 chemically links eq. 20 (or equivalently, eq. 13) (the pH^*-dependent, aqueous

$$t\text{-}(O)(HO)Re^{IV}L_4^{+} + e^{-} + H^{+} \rightarrow t\text{-}(HO)_2ReL_4^{+} \qquad \textbf{(20)}$$

reduction of Re^{IV}; Figures 5-7) with eq. 14 (or 4) (the pH^*-independent, nonaqueous reduction of Re^{IV}). Thus, the formal potentials for the aqueous and nonaqueous reactions should coincide at the pH^* value where $(HO)(MeO)Re^{III}L_4^+$ deprotonates (i.e. eq. 19). Extrapolation of the available Pourbaix plots yields pK_a values of ca. +22 to +26 (see Table VII).

In principle one should be able to use the remaining nonaqueous data to estimate pK_a's in other oxidation states. Unfortunately, the required auxiliary data for completion of the appropriate thermochemical cycles (e.g. pK_a for $(HO)(MeO)Re^{V}L_4^{3+}$, E_f for dioxorhenium(V/IV), etc.) are missing, and seemingly experimentally inaccessible. Some of these quantities would become accessible, however, if dimethoxo complexes (i.e. models for dihydroxo complexes) were available. As noted above, oxo,methoxorhenium(V) species resist further methylation. The corresponding Re(IV) species, on the other hand, might prove sufficiently electron rich to add a second methyl cation. Presumably the needed reactants could be generated by controlled potential electrolysis of $(O)(MeO)Re^{V}L_4^+$species in dry, oxygen-free organic solvents. We have not yet, however, explored this possibility experimentally.

Conclusions

High-valent, high-stability oxo,methoxo rhenium complexes can be prepared from the corresponding *trans*-dioxorhenium complexes and methyl trifluoromethane-sulfonate. The new complexes behave nearly identically, in an electrochemical and spectroscopic sense, to the analogous oxo, hydroxo complexes

— with one important exception: CH_3^+, unlike H^+, does not dissociate from the oxo ligand. The availability of a nonlabile proton analog permits one of the two usual proton-transfer steps to be disconnected from the usual 2-electron reductions of rhenium(V) species. As a result, the ordinarily inaccessible Re(IV) state is stabilized relative to Re(III) and Re(V) and becomes electrochemically accessible at high pH"s. The observation of the intermediate state is tremendously useful because it permits the stepwise thermodynamics of multi-electron, multi-proton transfer reactions to be mapped. This, in turn, is of central significance in correspondin[illegible] kinetic studies. Additionally, the oxo,methoxorhenium species can be used to obtain approximate thermodynamic information (acid dissociation constants) for ordinarily inaccessible complexes of the type $(O)(HO)Re^{VI}L_4^{3+}$, as well as for $(HO)Re^{III}L_4^+$ complexes.

References

1. Representative studies involving ruthenium: (a) Adeyemi, A.S.; Dovletoglou, A.; Gaudalupe, A.R.; Meyer, T.J. Inorg.Chem. 1992, 31, 1375. (b) Marmion, M.E.; Takeuchi, K.J. J.Am.Chem.Soc. 1988, 110, 1472. (c) Che, C.M.; Tang, W.T., Wong, W.T.; Lai, T.F. J.Am.Chem.Soc. 1989, 111, 9048. (d) Blaho, J.K.; Goldsby, K.A. J.Am.Chem.Soc. 1990, 112, 6132.

2. Representative studies involving osmium: (a) Pipes, D.W.; Meyer, T.J. Inorg.Chem. 1986, 25, 4042. (b) Takeuchi, K.J.; Thompson, M.S.; Pipes, D.W.; Meyer, T.J. Inorg.Chem. 1884, 23, 1845. (c) Dobson, J.C.; Takeuchi. K.J.; Pipes, D.W.; Geselowitz, D.A.; Meyer, T.J. Inorg.Chem. 1986, 25, 2357.

3. Representative studies involving manganese: (a) Thorp, H.H.; Sarneski, J.E.; Brudvig, G.W.; Crabtree, R.H. J.Am.Chem.Soc. 1989, 111, 9249. (b) Chan, M.K.; Armstrong, W.H. J.Am.Chem.Soc. 1989m 111, 9121. (c) Bradbury, J.R.; Schultz, F.A. Inorg.Chem. 1986, 25, 4408.

4. Studies involving rhenium: (a) Pipes, D.W.; Meyer, T.J. Inorg.Chem. 1986, 25, 3256. (b) Ram, M.S.; Johnson, C.S.; Blackbourn, R.L.; Hupp, J.T. Inorg.Chem. 1990, 2, 238. (c) Ram, M.S.; Jones, L.M.; Ward, H.J.; Wong, Y-H.; Johnson, C.S.; Subramanian, P.; Hupp, J.T. Inorg.Chem. 1991, 30, 2928. (d) Jones-Skeens, L.M.; Zhang, X.L.; Hupp, J.T. Inorg.Chem. 1992, 31, 3879.

5. Related studies involving dioxorhenium: (a) Winkler, J.R.; Gray, H.B. J.Am.Chem.Soc. 1993, 105, 1373. (b) Winkler, J.R.; Gray, H.B. Inorg.Chem. 1985, 24, 346. (c) Brewer, J.C.; Gray, H.B. Inorg.Chem. 1989, 28, 3334. (d)

Thorp, H.H.; Kumar, C.V.; Turro, N.J.; Gray, H.B. J.Am.Chem.Soc. 1989, 111, 4364. (e) Newsham, M.D. Giannelis, E.P.; Pinnavia, T.J.; Nocera, D.G. J.Am.Chem.Soc. 1988, 110, 3885. (f) Brewer, J.C.; Gray, H.B. *Reprints: Symposium on Selective Catalytic Oxidation of Hydrocarbons, ACS Division of Petroleum Chemistry, American Chemical Society:* Washington, D.C. 1990; pp. 187-191. (g) Johnson, C.S.; Mottley, C.; Hupp, J.T.; Donzer, G.I. Inorg.Chem. 1992, 31, 5143.

6. For recent discussions, see: (a) Thorp, H.H. J.Chem.Educ. 1992, 69, 250. (b) Thorp, H.H. Chemtracts: Inorg.Chem. 1991, 3, 171.

7. For reviews of metal-oxo chemistry; see: (a) Holm, R.H. Chem.Rev. 1987, 87, 1401 (b) Nugent, W.A.; Mayer, J.M. Metal-Ligand Multiple Bond; John Wiley and Sons: New York, 1988.

8. The doubly protonated Re(III) species could alternatively be represented as an aquo-oxo species.

9. For a somewhat dated but excellent review, see: Meyer, T.J. J.Electrochem.Soc. 1984, 131, 221c.

10. Reprensentative reports: (a) Gilbert, J.A.; Eggleston, D.S.; Murphy, W.R.; Geselowitz, D.A.; Gersten, S.W.; Hodgson, D.W.; Meyer, T.J. J.Am.Chem.Soc. 1985, 107, 3855. (b) Hurst, J.K.; Zhou, J.; Lei, Y. Inorg.Chem. 1992, 31, 1010.

11. Representative reports: (a) Dobson, J.C.; Seok, W.K.; Meyer, T.J. Inorg.Chem. 1986, 25, 1514. (b) Che, C.M.; Wong, K.Y.; Mak, T.C.

J.Chem.Soc.,Chem Commun. 1985, 988. (c) Groves, J.T.; Ahn, K.H. Inorg.Chem. 1987, 26, 381.

12. Representative reports: (a) Thompson, M.S.; Meyer, T.J. J.Am.Chem.Soc. 1982, 104, 4106. (b) McHatton, R.C.; Anson, F.C. 1984, 23, 3955.

13. For examples, however, of dioxorhenium-based electrocatalysis, see: Thorp, H.H.; Van Houten, J.; Gray, H.B. Inorg.Chem. 1989, 28, 889 and ref. 4a.

14. For related discussions of multi-ET kinetics see, for example: (a) Pfennig, B.W.; Bocarsly, A.B. Comm.Inorg.Chem. 1992, 13, 261. (b) Richardson, D.E.; Taube, H. Coord.Chem.Rev. 1984, 60, 107. (c) Ram, M.S.; Hupp, J.T. J.Phys.Chem. 1990, 94, 2378.

15. A mechanistic discrepancy between cyclic voltammetry and steady-state microelectrode findings was noted in ref. 4d, and tentatively ascribed to differences in reaction medium and pH and to other effects. We have since found, via extensive digital simulation studies, that the critical variable is the overpotential region (i.e. thermodynamic driving force region) in which the rate measurements are made. At the formal potential, reaction 4 is rate determining; at somewhat more negative potentials the rate is controlled by reaction 3.

16. Skeens-Jones, L.M., Ph.D. Dissertation, Northwestern University, 1992.

17. "Direct" to the extent that the oxo-hydroxo/oxo-methoxo analogy is valid.

18. Liu, W.; Welch, T.W.; Thorp, H.H. Inorg.Chem. 1992, 31, 4044.

19. Lu, H.; Skeens-Jones, L.M.; Hupp, J.T. unpublished results.

20. (a) Brewer, J.C.; Gray, H.B. Inorg.Chem. 1989, 28, 3344. (b) Ram, M.S.; Hupp, J.T. Inorg.Chem. 1991, 30, 130.

21. The TEXRAY Structure Analysis Program Packagem Molecular Structure Corporation, College Station, Texas, 1986.

22. (a) Johnson, J.W.; Brody, J.F.; Ansell, G.B.; Zentz, S. Inorg.Chem. 1984, 23, 2415. (b) Lock, C.J.L.; Turner, G. Acta Cryst. 1978, B34, 923. (c) Lock, C.J.L.; Turner, G. Can.J.Chem. 1977, 55, 333. (d) Calvo, C.; Krishnamacher, N.; Lock, C.J.L. J.Cryst.Mol.Struct. 1971, 1, 161.

23. Cotton, F.A. ; Lippard, S.J. Inorg.Chem. 1965, 4, 1621.

24. (a) Bakir, M.; Paulson, S.; Goodson, P.; Sullivan, B.P. Inorg.Chem. 1992, 31, 1129. (b) Forsellini, E.; Casellato, U.; Graziani, R.; Carletti, M.C.; Magon, L. Acta Crystallogr. 1984, C40, 1795. (c) Ciani, G.F.; D'Alfonso, G.; Romitiz, P.F.l Sironi, A.; Freni, M. Inorg.Chim.Acta 1983, 72, 29. (d) Haymore, B.L.; Goeden, G.V. Inorg.Chem. 1983, 22, 157.

25. (a) Paradis, J.A.; Wertz, D.W.; Thorp, H.H. J.Am.Chem.Soc. in press. (b) Ballhausen, C.J.; Gray, H.B. Inorg.Chem. 1962, 1, 111. (c) Hopkins, M.D.; Miskowski, V.M.; Gray, H.B. J.Am.Chem.Soc. 1986, 108, 6908.

26. From Table III we observe that the extinction coefficient for the d-d absorption increases (as expected) as the MLCT/d-d energy gap decreases.

27. In the majority of cases involving other (O)(MeO)ReL_4 species, the IV/III step was only quasi-reversible in an electrochemical kinetic sense (e.g. peak separations of ca. 200 mV at a sweep rate of 0.1 V/s). Apparently this

reduction entails somewhat larger internal mode displacements (activation barrier requirements) than do the VI → V and V → IV reductions. Reasonably accurate E_f values were still obtainable, however, by making measurements at very slow sweep rates.

28. Below $pH^* \approx 0$ the reactant is $(O)(HO)Re^{V}(Mepy)_4^{2+}$.

29. Sawada, M.; Ichihara, M.; Yukawa, Y.; Nakachi, T.; Tsumo, Y. Bull.Chem.Soc.Jpn. 1980, 53, 2055.

30. It is conceivable, based on the oxo,methoxo results, that the proton-decoupled dioxorhenium(V/IV) formal potential lies negative of the (presumably) irreversible reduction potential of ligated pyridine derivatives.

31. Oxo,*phen*oxides of rhenium(V) have also been prepared (by using benzylbromide as an aryl cation source). These species are similar, both electrochemically and spectroscopically, to the oxo, methoxo complexes described here. (Ram, M.S., unpublished results.)

32. Hupp, J.T.; Zhang X.L., work in progress (see also, ref. 4d).

Table I. Summary of Crystal Struture Data for $[(O)(MeO)Re(Me_2py)_4](CF_3SO_3)_2 \bullet CH_3COCH_3$.

Formula	$ReS_2O_9F_6N_4C_{34}H_{45}$
M	1018.07
cryst. size, mm	0.490 X 0.082 x 0.042
cryst. system	monoclinic
space group	$P2_1/c$ (#14)
a, Å	15.256 (2)
b, Å	20.604 (3)
c, Å	12.976 (4)
β, deg	90.41 (2)
V, Å^3	4079 (3)
Z	4
d_{calcd}, g cm^{-3}	1.658
μ(Mo-Kα), cm^{-1}	31.96
radiation	graphite - mponochromated Mo-Kα (λ = 0.71069 Å)
scan type	ω-Θ
2Θ range, deg	4-47
scan width, deg	(1.00 + 0.35 tanΘ)°
unique data	6231
unique date with I>3σ(I)	3365
no. of parameters	461
R(F)	0.047
R_w(F)	0.049
GOF	1.50

Table II. Selected Bond Distances (Å) and Angles (deg) for $[(O)(MeO)Re(Me_2py)_4](CF_3SO_3)_2$

Re — O1	1.829(7)
Re — O2	1.693(7)
Re — N1	2.131(8)
Re — N2	2.1458)
Re — N3	2.138(9)
Re — N4	2.136(9)
O1 — CO1	1.44(1)
O1 — Re — O2	177.6(3)
Re — O1 — CO1	172.1(7)
O1 — Re — N1	89.3(3)
O1 — Re — N2	90.5(3)
O1 — Re — N3	87.8(4)
O1 — Re — N4	88.3(3)
O2 — Re — N1	92.7(4)
O2 — Re — N2	90.9(3)
O2 — Re — N3	90.2(4)
O2 — Re — N4	90.3(3)
N1 — Re — N2	89.4(3)
N1 — Re — N3	176.8(4)
N1 — Re — N4	88.1(3)
N2 — Re — N3	92.0(3)
N2 — Re — N4	177.2(3)
N3 — Re — N4	90.5(3)

Table III. Electronic Absorption Spectral Data for Oxo-Methoxo, Oxo-Hydroxo and Dioxo Rhenium(V) Complexes

Complex	λ_{max},nm(ε,$M^{-1}cm^{-1}$)		
$(O)(MeO)Re(pyrrpy)_4^{2+}$	265(3.9×10^4)	314(6.5×10^4)	569(1.7×10^3)
$(O)(HO)Re(pyrrpy)_4^{2+,b}$	267(5.2×10^4)	315(5.2×10^4)	574(1.7×10^3)
$(O)_2Re(pyrrpy)_4^{+}$	273(5.2×10^4)	353(4.2×10^4)	465(2.6×10^3)
$(O)(MeO)Re(dmap)_4^{2+}$	262(3.3×10^4)	313(5.7×10^4)	565(1.7×10^3)
$(O)(HO)Re(dmap)_4^{2+,b}$	261(2.4×10^4)	315(5.1×10^4)	568(1.3×10^3)
$(O)_2Re(dmap)_4^{+}$	272(4.7×10^4)	358(3.7×10^4)	462(2.3×10^3)
$(O)(MeO)Re(py)_2(dmap)_2^{2+}$		295(3.4×10^4)	531(1.5×10^3)
$(O)(HO)Re(py)_2(dmap)_2^{2+}$		305(4.6×10^4)	533(1.7×10^3)
$(O)_2Re(py)_2(dmap)_2^{+}$	253(1.7×10^4)	363(1.0×10^4)	471(1.6×10^3)
$(O)(MeO)Re(MeOpy)_4^{2+}$		271(2.9×10^4)	521(9.0×10^2)
$(O)(HO)Re(MeOpy)_4^{2+,d}$		276(2.9×10^4)	521(9.0×10^2)
$(O)_2Re(MeOpy)_4^{+}$	281(7.0×10^3)	347(2.7×10^4)	438(1.5×10^3)
$(O)(MeO)Re(Me_2py)_4^{2+}$		281(1.7×10^4)	511(7.0×10^2)
$(O)(HO)Re(Me_2py)_4^{2+}$		284(1.2×10^4)	510(6.4×10^2)
$(O)_2Re(Me_2py)_4^{+}$	275(5.7×10^3)	356(2.9×10^4)	416(2.1×10^3)
$(O)(MeO)Re(Mepy)_4^{2+}$		280(1.5×10^4)	508(7.2×10^2)
$(O)_2Re(Mepy)_4^{+}$	247(1.6×10^4)	353(3.2×10^4)	429(2.0×10^3)

[a]Solvent is 50:50 $CH_3CN:H_2O$. [b]0.5 M H_2SO_4 (50:50 $CH_3CN:H_2O$). Higher acid concentrations led to decomposition. [c]2.0 M H_2SO_4 (50:50 $CH_3CN:H_2O$).

Table IV. Aqueous Redox Potentials ($pH^* = 7.8$) for *t*-$(O)(OMe)ReL_4^{2+}$ and *t*-$(O)_2ReL_4^+$ Complexes.

Complex	E_f(V/III)[a,b]
$(O)(MeO)Re(4\text{-}pyrrpy)_4^{m+}$	-0.87
$(O)_2Re(pyrrpy)_4^{n+}$	-1.00[c]
$(O)(MeO)Re(dmap)_4^{m+}$	-0.86
$(O)_2Re(dmap)_4^{n+}$	-1.03[c]
$(O)(MeO)Re(py)_2(dmap)_2^{m+}$	-0.76
$(O)_2Re(py)_2(dmap)_2^{n+}$	-0.97[c]
$(O)(MeO)Re(MeOpy)_4^{m+}$	-0.73
$(O)_2Re(MeOpy)_4^{n+}$	-0.97[c]
$(O)(MeO)Re(Me_2py)_4^{m+}$	-0.72
$(O)_2Re(Me_2py)_4^{n+}$	-.096[c]
$(O)(MeO)Re(Mepy)_4^{m+}$	-0.71
$(O)_2Re(Mepy)_4^{n+}$	-0.96[c]

a. Formal potentials in 50:50 $CH_3CN:H_2O$ buffered at $pH^* = 7.8$. b. In volts vs s.s.c.e. c. Data taken from ref. 4c.

Table V. Nonaqueous Redox Potentials for *t*-(O)(MeO)ReL_4^{m+} and *t*-$(O)_2ReL_4^{n+}$ Complexes.

Complex	E_f(VI/V)[a,b]	E_f(V/IV)[a,b]	E_f(IV/III)[a,b]
$(O)(MeO)Re(4\text{-}pyrrpy)_4^{m+}$	1.30	-1.08	-1.75
$(O)_2Re(pyrrpy)_4^{n+}$	0.55		
$(O)(MeO)Re(dmap)_4^{m+}$	1.39	-1.08	-1.83
$(O)_2Re(dmap)_4^{n+}$	0.53		
$(O)(MeO)Re(py)_2(dmap)_2^{m+}$	1.61	-0.86	-1.72
$(O)_2Re(py)_2(dmap)_2^{n+}$	0.86		
$(O)(MeO)Re(MeOpy)_4^{m+}$	1.98	-0.81	-1.78
$(O)_2Re(MeOpy)_4^{n+}$	1.04		
$(O)(MeO)Re(Me_2py)_4^{m+}$	2.12	-0.77	-1.60
$(O)_2Re(Me_2py)_4^{n+}$	1.17		
$(O)(MeO)Re(Mepy)_4^{m+}$	2.20	-0.74	-1.60
$(O)_2Re(Mepy)_4^{n+}$	1.12		

a. Formal potentials in acetonitrile with 0.1 M $TBAPF_6$ electrolyte. b. In volts vs. s.s.c.e.

Table VI. Estimated pK_a Values for $(O)(HO)Re^{VI}L_4^{3+}$ Complexes

Complex	$pK_a(VI)^a$
$(O)(HO)Re(pyrrpyr)_4^{3+}$	-10.4[b]
$(O)(HO)Re(dmap)_4^{3+}$	-12.3[c]
$(O)(HO)Re(py)_2(dmap)_2^{3+}$	-12[c]
$(O)(HO)Re(MeOpy)^{3+}$	-15.4[c]
$(O)(HO)Re(Me_2py)_4^{3+}$	-16[d]
$(O)(HO)Re(Mepy)_4^{3+}$	-18[d]

a. Estimated via eq.17; see text. b. Required pK_a for $(O)(HO)Re^{V}(pyrrpyr)_4^{2+}$ assumed to equal that for $(O)(HO)Re^{V}(dmap)_4^{2+}$. c. Required pK_a for $(O)(HO)Re^{V}L_4^{2+}$ taken from ref. 4c. d. Required pK_a for $(O)(HO)Re^{V}L_4^{2+}$ estimated on the basis of pyridyl (free ligand)/hydroxol(bound ligand) acidity correlation reported in ref. 4c.

Table VII. Estimated pK_a Values (first pK_a) for $(HO)_2Re^{III}L_4^+$ Species.

Complex	pK_a [a]
$(HO)_2Re^{III}(pyrrpy)_4^+$	24
$(HO)_2Re^{III}(dmap)_4^+$	26
$(HO)_2Re^{III}(py)_2(dmap)_2^+$	25
$(HO)_2Re^{III}(MeOpy)_4^+$	25
$(HO)_2Re^{III}(Me_2py)_4^+$	22
$(HO)_2Re^{III}(Mepy)_4^+$	23

a. Estimated from oxo,methoxorhenium electrochemical data as described in text.

b. Pourbaix slope for reaction 19b (required for pK_a estimation) not directly measured for this complex, but assumed to equal 59 mV per pH^* unit.

Figure captions

1. ORTEP drawing of *t*-(O)(MeO)Re(Me_2py)$_4^{2+}$.
2. UV-visible spectra *t*-(O)(MeO)Re(Me_2py)$_4^{2+}$ (solid line) and *t*-(O)(HO)Re(Me_2py)$_4^{2+}$ (dashed line) in 50:50 CH_3CN:H_2O with 2 M H_2SO_4..
3. Resonance Raman spectra (514.5 nm excitation) of *t*-(O)(MeO)Re(dmap)$_4^{2+}$ (top) and *t*-(O)(MeO)Re(Me_2py)$_4^{2+}$ (bottom) in 50:50 CH_3CN:water at pH* = 7.7. Asterisks denote solvent peaks.
4. Background-subtracted cyclic voltammograms (sweep rate = 100 mV/s) for the reduction and re-oxidation of *t*-(O)(MeO)Re(dmap)$_4^{2+}$ (solid line) and *t*-$(O)_2$Re(dmap)$_4^{+}$ dashed line in 50:50 CH_3CN:water at pH* = 8.0.
5. Pourbaix diagram for *t*-$(O)_2$Re(MeOpy)$_4^{+}$ in 50:50 CH_3CN:water.
6. Pourbaix diagrams for *t*-(O)(MeO)Re$(py)_2$(dmap)$_2^{2+}$ (top), *t*-(O)(MeO)Re(MeOpy)$_4^{2+}$ (middle) and *t*-(O)(MeO)Re(Me_2py)$_4^{2+}$ (bottom) in 50:50 CH_3CN:water.
7. Pourbaix diagrams for *t*-(O)(MeO)Re(pyrrpy)$_4^{2+}$ (top) and *t*-(O)(MeO)Re(dmap)$_4^{2+}$ (bottom) in 50:50 CH_3CN:water.
8. Pourbaix diagrams for *t*-$(O)_2$Re(Me_2py)$_4^{+}$ (top), *t*-$(O)_2$Re$(py)_2$(dmap)$_2^{+}$ (middle) and *t*-$(O)_2$Re(pyrrpy)$_4^{+}$ (bottom) in 50:50 CH_3CN:water.
9. Cyclic voltammogram (sweep rate = 1 V/s) for *t*-(O)(MeO)Re(Mepy)$_4^{2+}$ in acetonitrile with 0.1M $TBAPF_6$ as electrolyte.
10. Formal potentials in acetonitrile for *t*-(O)(MeO)Re$L_4^{3+/2+/1+/0}$ versus free ligand (L) basicity. Key to ligands: 1) pyrrpy 2) dmap, 3) py + dmap, 4) MeOpy, 5) Me_2py, 6)Mepy.

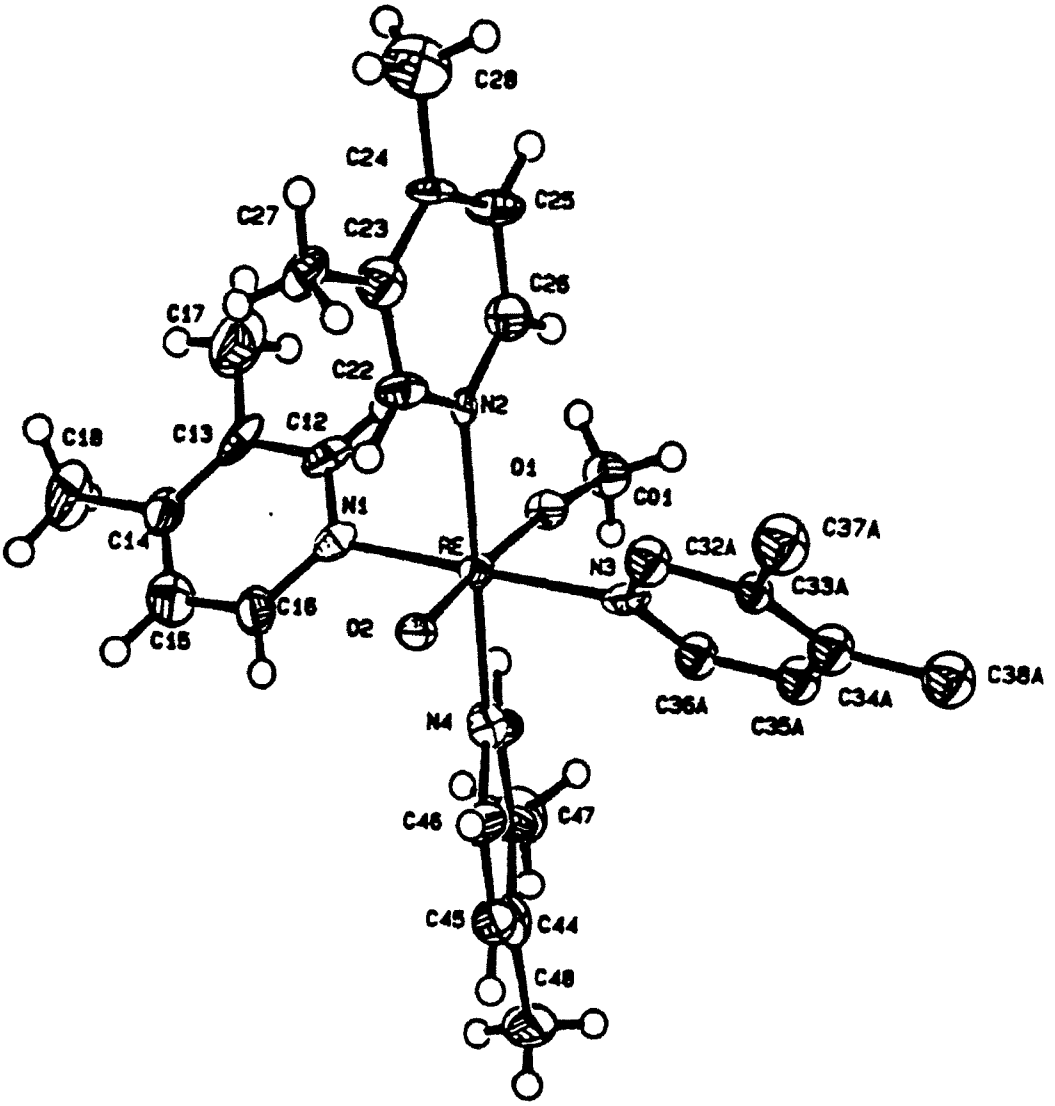
C28
C24
C25
C27
C23
C26
C17
C22
N2
C18
C13
C12
O1
C01
N1
C14
RE
C37A
C32A
N3
C33A
C16
C15
O2
C38A
C36A
C34A
C35A
N4
C46
C47
C45
C44
C48

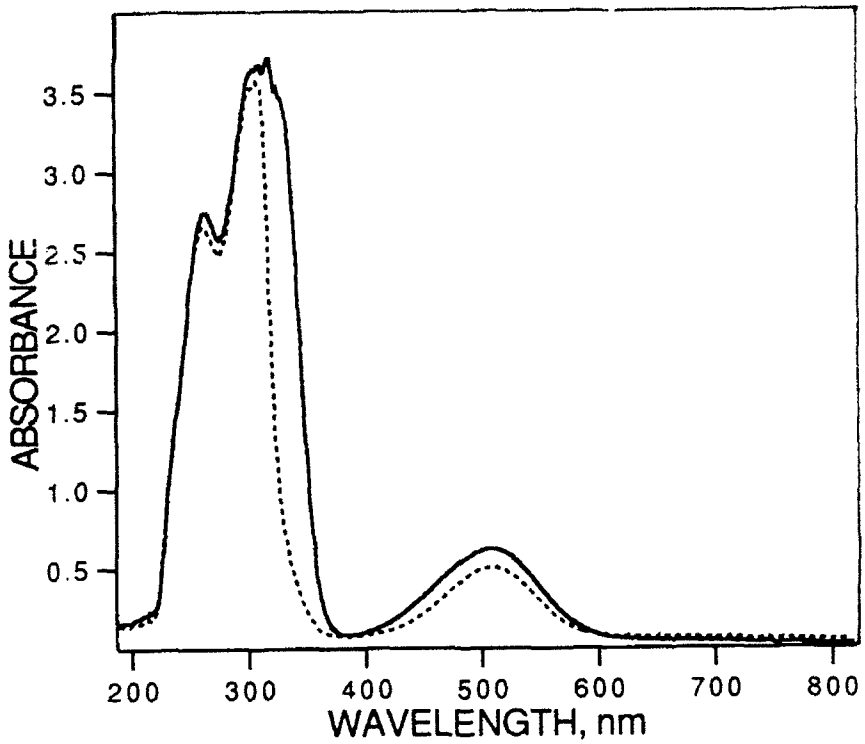
ABSORBANCE
3.5
3.0
2.5
2.0
1.5
1.0
0.5
200
300
400
500
600
700
800
WAVELENGTH, nm

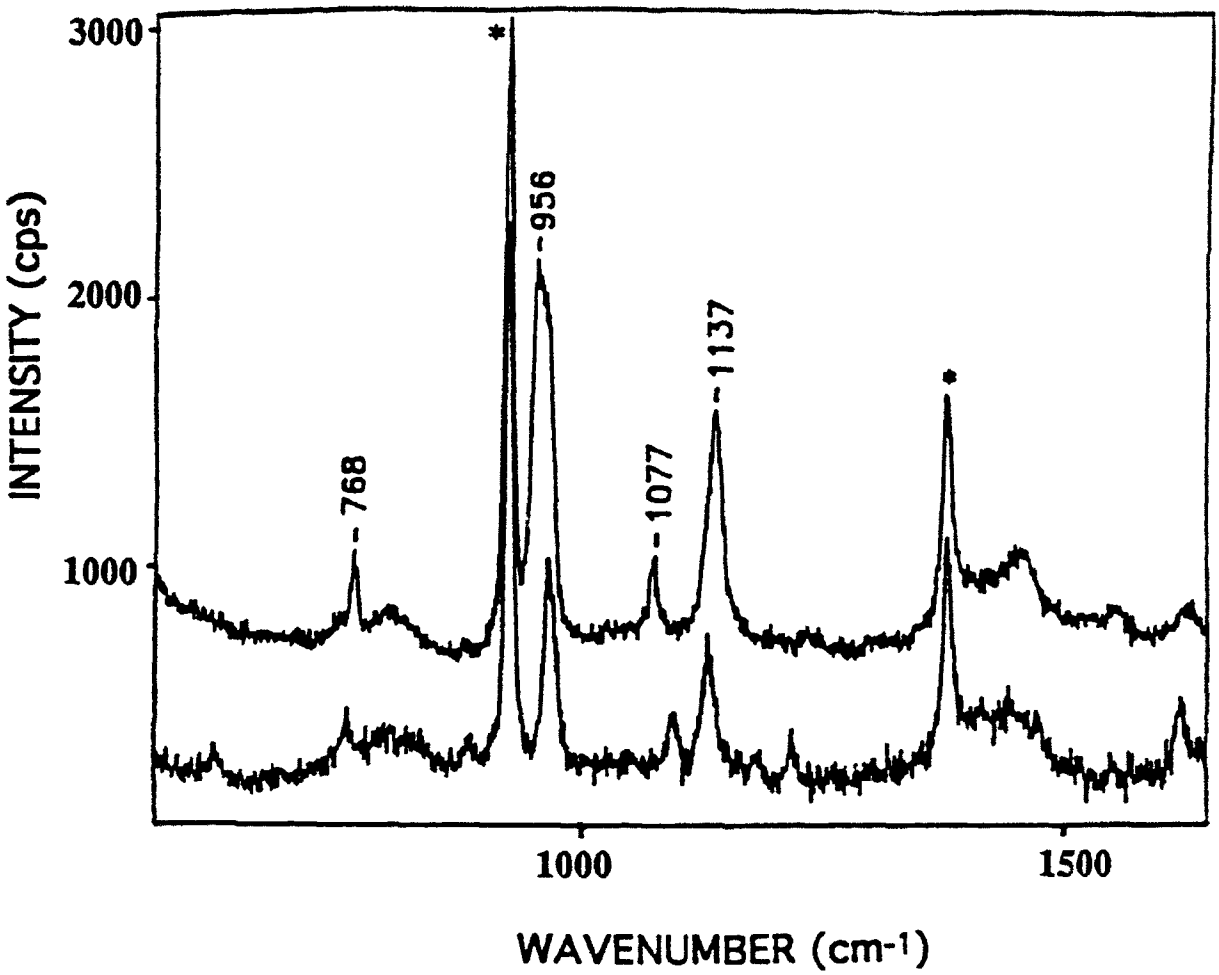
3000
2000
1000
INTENSITY (cps)
768
956
1077
1137
*
*
1000
1500
WAVENUMBER (cm-1)

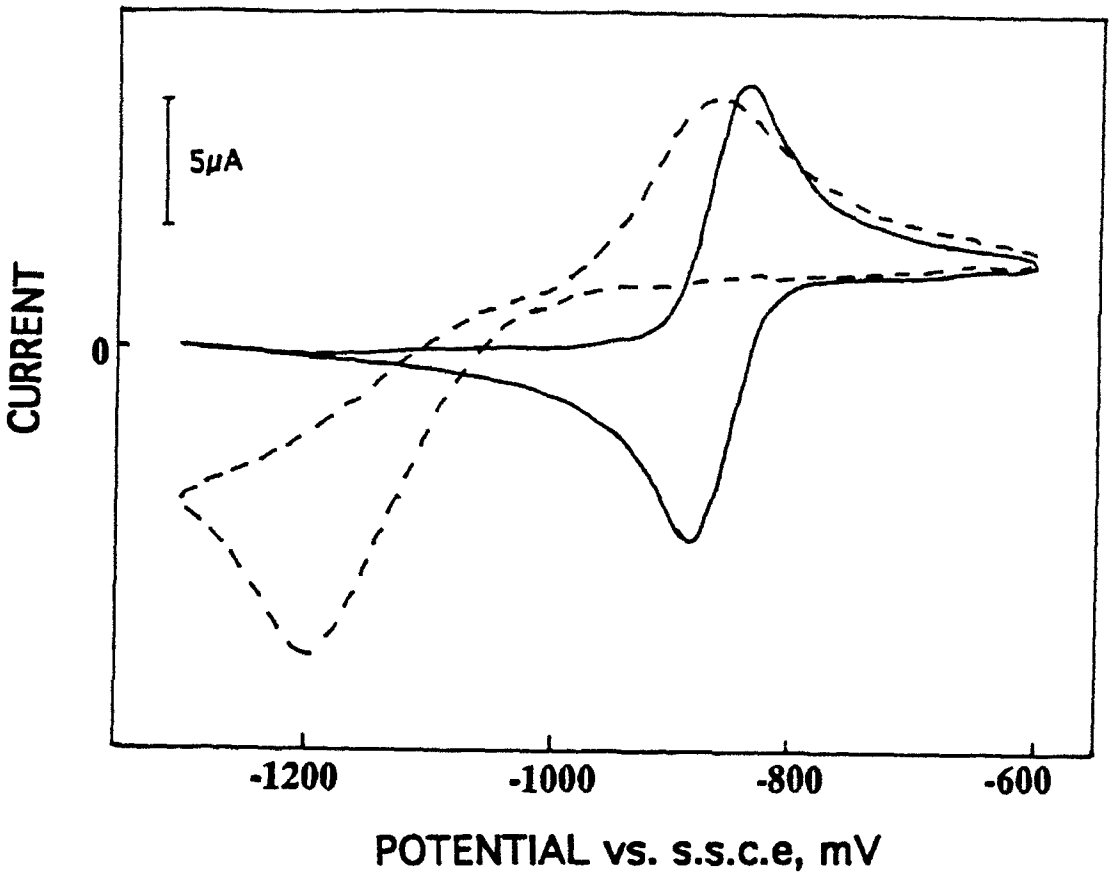
5μA
CURRENT
0
-1200
-1000
-800
-600
POTENTIAL vs. s.s.c.e, mV

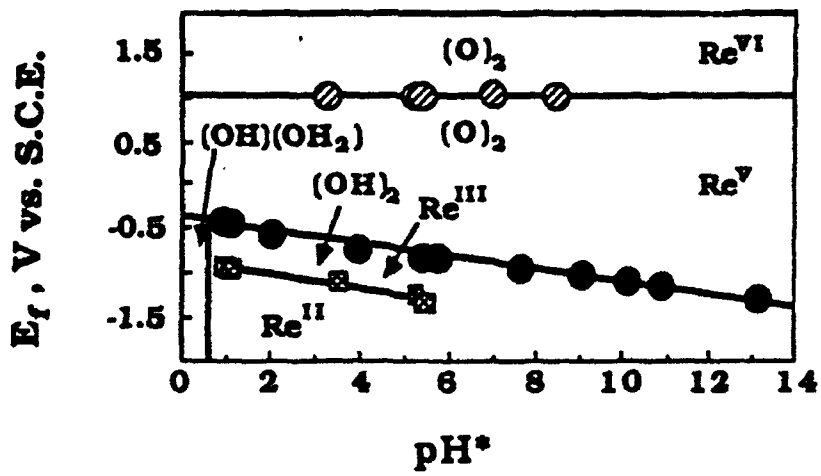
1.5
0.5
-0.5
-1.5
0
2
4
6
8
10
12
14
E_f, V vs. S.C.E.
pH*
$(O)_2$
Re^{VI}
$(OH)(OH_2)$
$(O)_2$
$(OH)_2$
Re^{III}
Re^{V}
Re^{II}

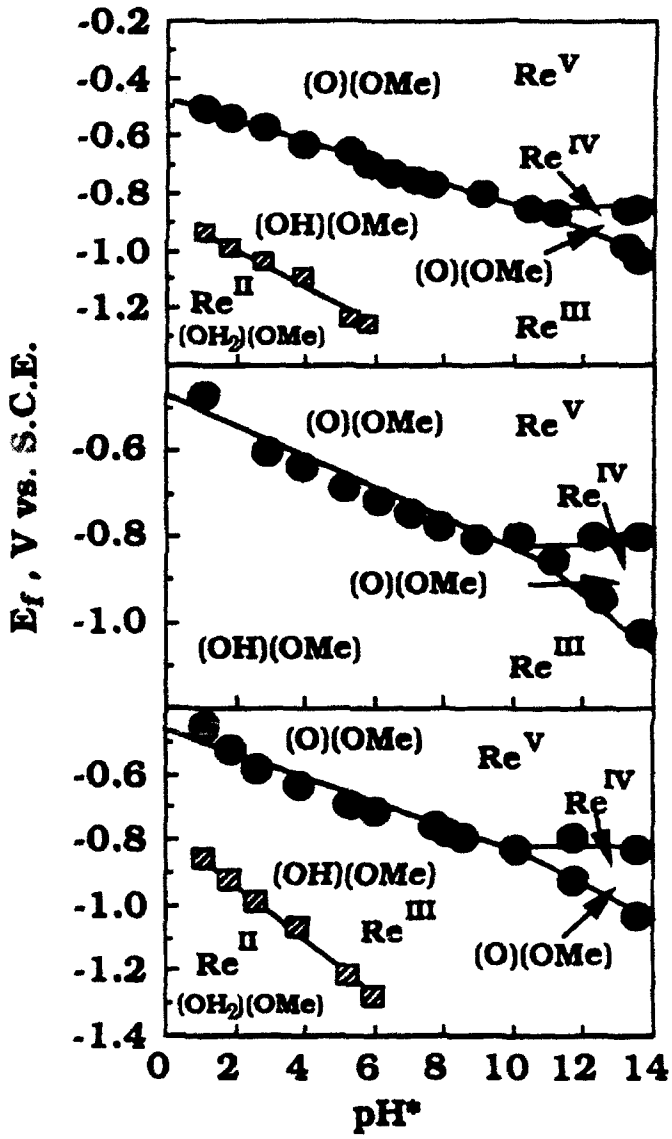
-0.2
-0.4
-0.6
-0.8
-1.0
-1.2
(O)(OMe)
Re V
Re IV
(OH)(OMe)
(O)(OMe)
Re II
(OH2)(OMe)
Re III
-0.6
-0.8
-1.0
(O)(OMe)
Re V
Re IV
(O)(OMe)
(OH)(OMe)
Re III
-0.6
-0.8
-1.0
-1.2
-1.4
(O)(OMe)
Re V
Re IV
(OH)(OMe)
Re III
Re II
(O)(OMe)
(OH2)(OMe)
0 2 4 6 8 10 12 14
pH*
Ef , V vs. S.C.E.

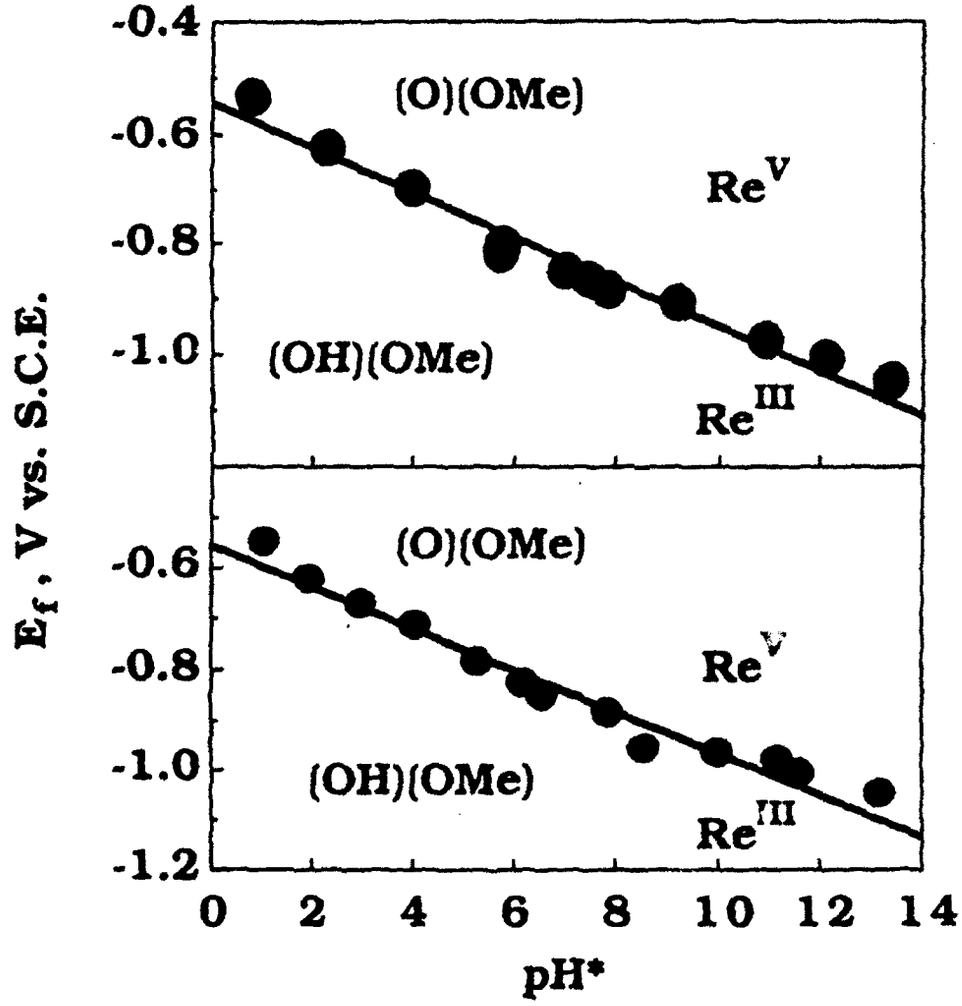
-0.4
-0.6
-0.8
-1.0
(O)(OMe)
Re^V
(OH)(OMe)
Re^III
-0.6
-0.8
-1.0
-1.2
(O)(OMe)
Re^V
(OH)(OMe)
Re^III
0
2
4
6
8
10
12
14
pH*
E_f , V vs. S.C.E.

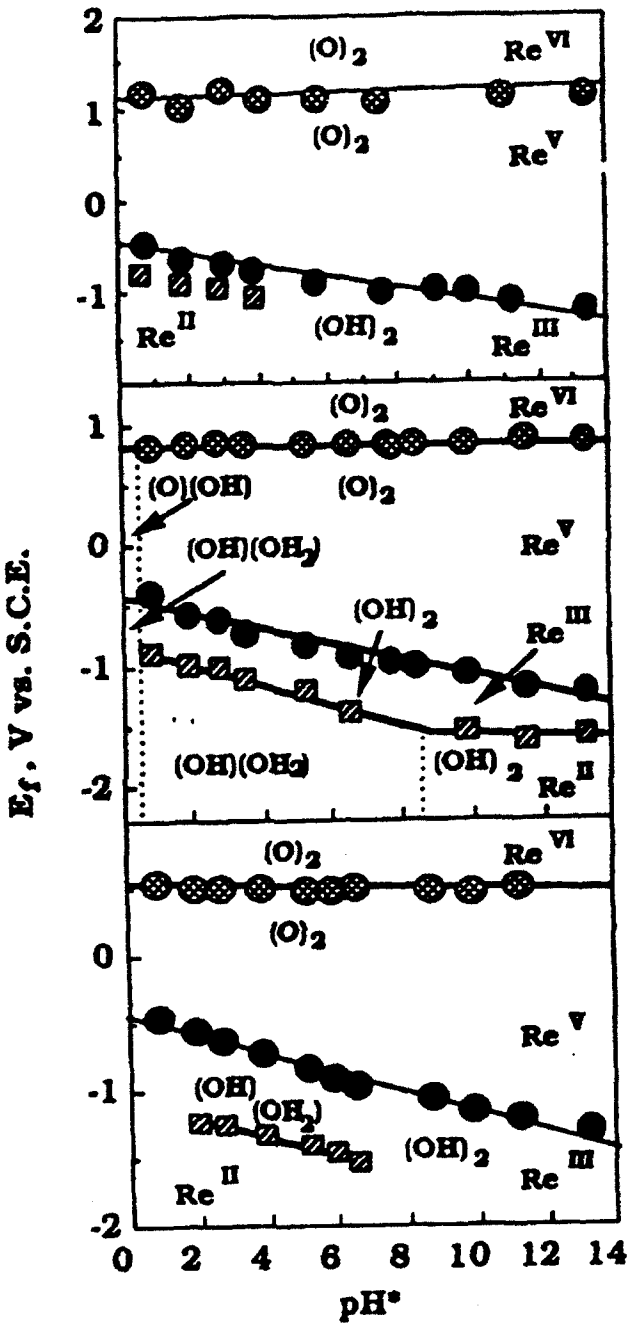
2
1
0
-1
-2
$(O)_2$
Re^{VI}
$(O)_2$
Re^{V}
Re^{II}
$(OH)_2$
Re^{III}
$(O)_2$
Re^{VI}
(O)(OH)
$(O)_2$
Re^{V}
$(OH)(OH_2)$
$(OH)_2$
Re^{III}
$(OH)(OH_2)$
$(OH)_2$
Re^{II}
$(O)_2$
Re^{VI}
$(O)_2$
Re^{V}
(OH)
(OH_2)
$(OH)_2$
Re^{III}
Re^{II}
E_f, V vs. S.C.E.
0 2 4 6 8 10 12 14
pH*

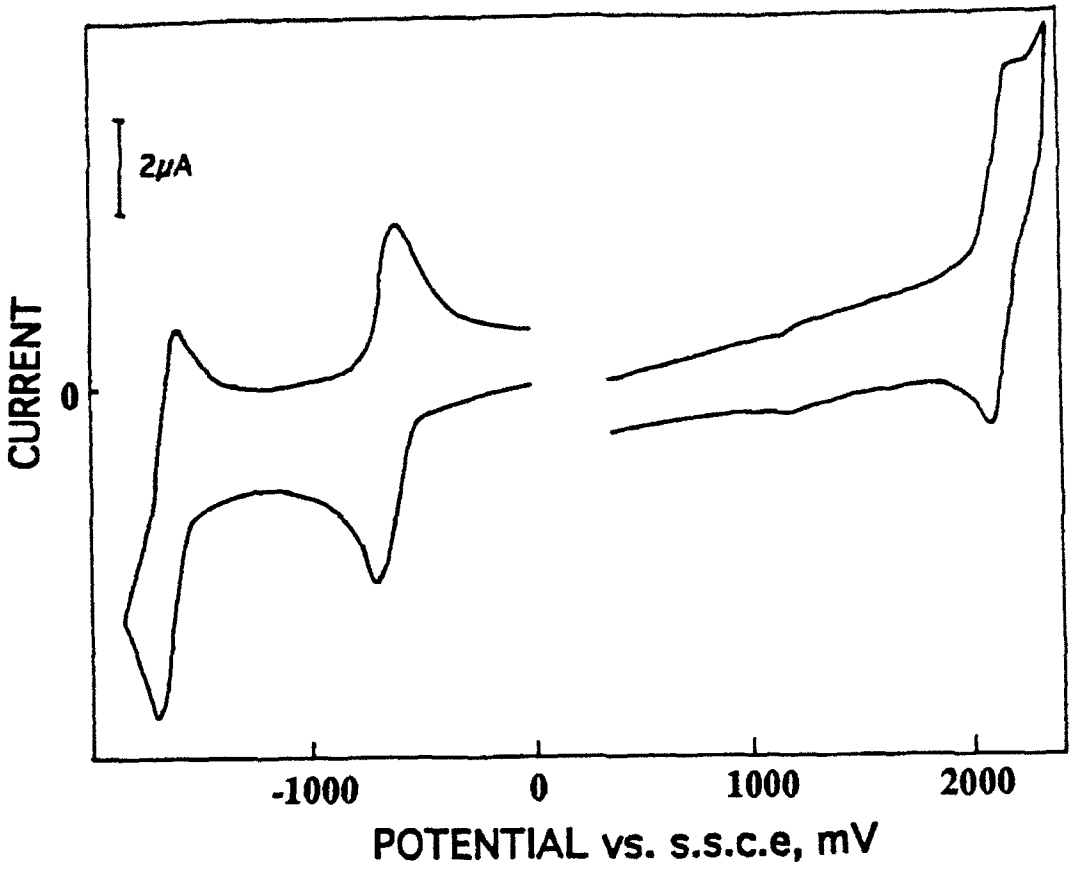
2μA
CURRENT
0
-1000
0
1000
2000
POTENTIAL vs. s.s.c.e, mV

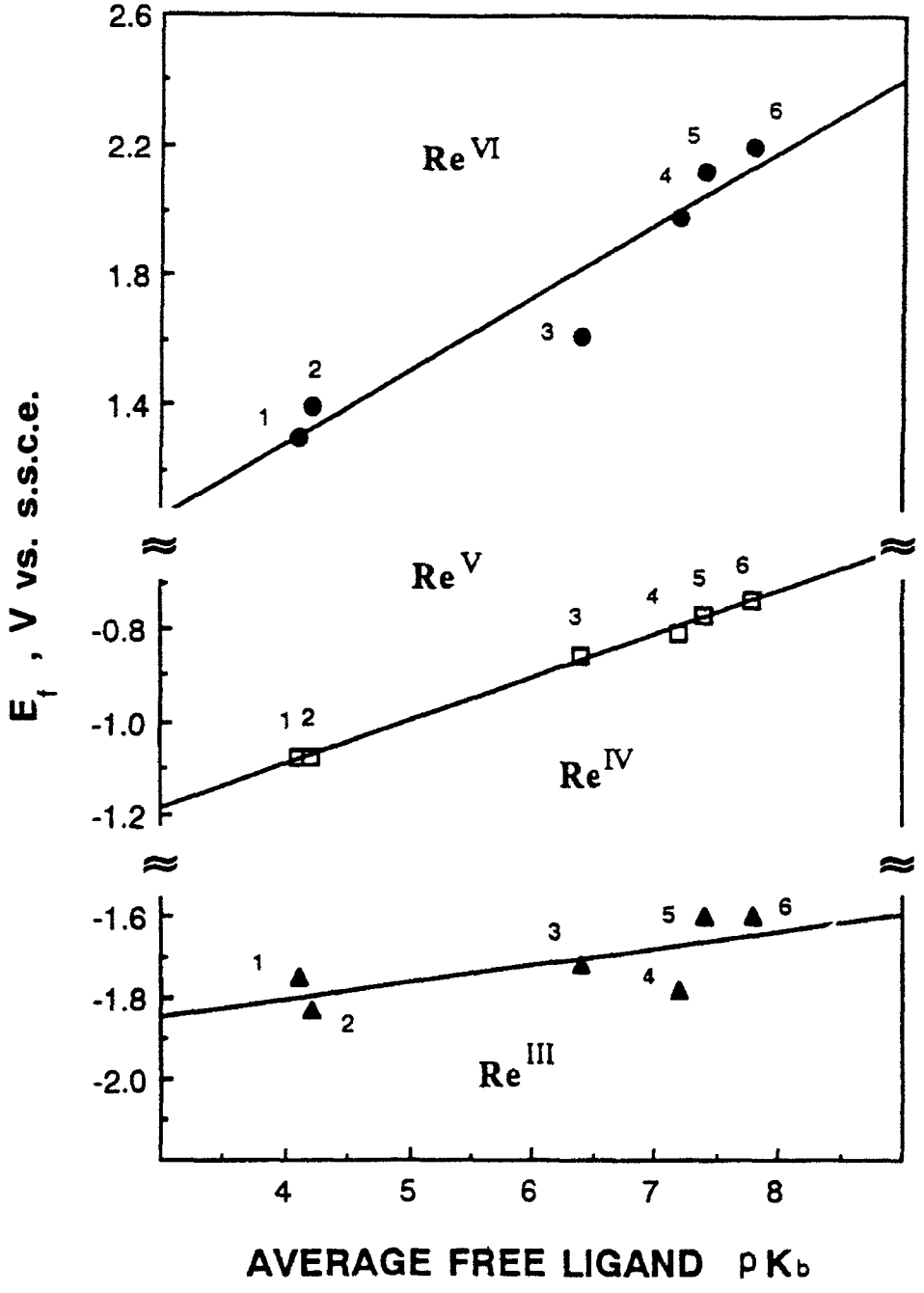
2.6
2.2
1.8
1.4
Re VI
1
2
3
4
5
6
-0.8
-1.0
-1.2
Re V
Re IV
1 2
3
4
5
6
-1.6
-1.8
-2.0
Re III
1
2
3
4
5
6
4
5
6
7
8
E f , V vs. s.s.c.e.
AVERAGE FREE LIGAND pKb